

Bandgap Engineering of Strained Monolayer and Bilayer MoS₂

Hiram J. Conley,[†] Bin Wang,[†] Jed I. Ziegler,[†] Richard F. Haglund Jr.,[†] Sokrates T. Pantelides,^{†,‡} and Kirill I. Bolotin^{*,†}

Department of Physics and Astronomy, Vanderbilt University, and Materials Science and Technology Division, Oak Ridge National Laboratory

E-mail: kirill.bolotin@vanderbilt.edu

KEYWORDS: MoS₂, strain, bandgap engineering, photoluminescence, Grüneisen parameter

Abstract

We report the influence of uniaxial tensile mechanical strain in the range 0–2.2% on the phonon spectra and bandstructures of monolayer and bilayer molybdenum disulfide (MoS₂) two-dimensional crystals. First, we employ Raman spectroscopy to observe phonon softening with increased strain, breaking the degeneracy in the E' Raman mode of MoS₂, and extract a Grüneisen parameter of ~ 1.06 . Second, using photoluminescence spectroscopy we measure a decrease in the optical band gap of MoS₂ that is approximately linear with strain, ~ 45 meV/% strain for monolayer MoS₂ and ~ 120 meV/% strain for bilayer MoS₂. Third, we observe a pronounced strain-induced decrease in the photoluminescence intensity of monolayer MoS₂ that is indicative of the direct-to-indirect transition of the character of the optical band gap of this material at applied strain of $\sim 1\%$. These observations constitute the first demonstration of strain engineering the band structure in the emergent class of two-dimensional crystals, transition-metal dichalcogenides.

^{*}To whom correspondence should be addressed

[†]Department of Physics and Astronomy, Vanderbilt University

[‡]Materials Science and Technology Division, Oak Ridge National Laboratory

Monolayer¹ molybdenum disulfide (MoS₂), along with other monolayer transition metal dichalcogenides (MoSe₂, WS₂, WSe₂) have recently been the focus of extensive research activity that follows the footsteps of graphene, a celebrated all-carbon cousin of MoS₂.¹ Unlike semimetallic graphene, monolayer MoS₂ is a semiconductor with a large direct band gap.^{2,3} The presence of a band gap opens a realm of electronic and photonic possibilities that have not been previously exploited in two-dimensional crystals and allows fabrication of MoS₂ transistors with an on/off ratio exceeding 1×10^8 ,^{4,5} photodetectors with high responsivity,⁶ and even LEDs.⁷ Moreover, the direct nature of the band gap causes MoS₂ to exhibit photoluminescence at optical wavelengths^{2,3} with intensity that is tunable via electrical gating.⁸⁻¹⁰ Finally, strong Coulomb interactions between electrons and holes excited across the band gap of MoS₂ lead to the formation of tightly bound excitons that strongly affect the optical properties of this material.^{9,10}

It has been well established that straining a two dimensional material shifts its phonon modes, allowing a simple method to detect strain in these materials. These shifts, that are due to the anharmonicity of molecular potentials, can be probed with micro-Raman spectroscopy.^{11,12} Very recently, it has been proposed that mechanical strain can strongly perturb the band structure of MoS₂. It has been predicted that straining MoS₂ modifies the band gap energy and the carrier effective masses. Moreover, at strains larger than 1% the lowest lying band gap changes from direct to indirect.¹³⁻¹⁸ It has been suggested that strain engineering of the band structure of MoS₂ could be used to increase carrier mobility of MoS₂, to create tunable photonic devices and solar cells,¹⁹ and even to control the magnetic properties of MoS₂.^{13,14} While strain perturbs the band structure of all materials, two-dimensional materials such as MoS₂ can sustain strains greater than 11%,²⁰ allowing exceptional control of material properties by strain engineering.

Here, we investigate the influence of uniaxial tensile strain from 0% to 2.2% on the phonon spectra and band gaps of both monolayer and bilayer MoS₂, by employing a four point bending apparatus (Fig. 1). First, with increasing strain, for both mono- and bilayer MoS₂ we observe splitting of the Raman peak due to the E' phonon mode into two distinct peaks that shift by 4.5

¹Monolayer in this paper refers to one *molecular* molybdenum disulfide (MoS₂) layer, or one layer of molybdenum atoms sandwiched between two layers of sulphur atoms. It is also sometimes referred to as trilayer MoS₂.

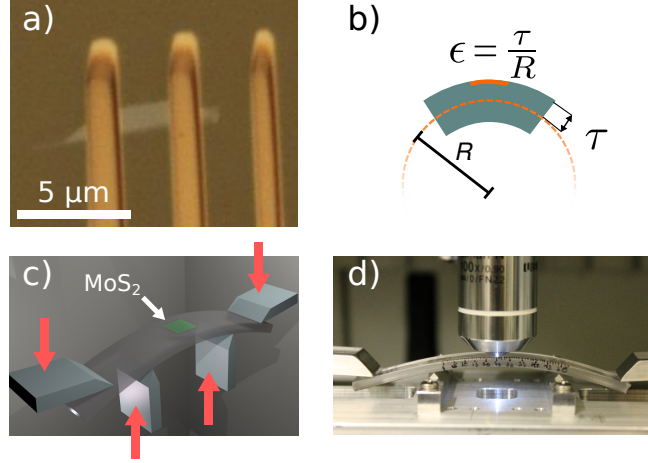


Figure 1: **Straining MoS₂ devices** (a) Optical image of a bilayer MoS₂ flake with titanium clamps attaching it to SU8/polycarbonate substrate. (b,c) Schematic of the beam bending apparatus used to strain MoS₂. (d) Photograph of bending apparatus with MoS₂ under strain.

and $1 \text{ cm}^{-1}/\%$ strain. Second, a linear redshift of $45 \text{ meV}/\%$ strain of the position of the A peak in photoluminescence for monolayer MoS₂ ($53 \text{ meV}/\%$ strain for bilayer MoS₂) indicates a corresponding reduction in band gap energy of these materials. Finally, we observe a pronounced strain-induced decrease in intensity of the photoluminescence of monolayer MoS₂. Our modelling and first-principles calculations indicate that this decrease is consistent with a transition of an optical band gap of MoS₂ from direct to indirect at $\sim 1\%$ strain, while the fundamental (or transport) band gap remains direct in the investigated regime of strain.

Fabrication of controllably strained devices starts by mechanically exfoliating²¹ MoS₂ onto a layer of cross-linked SU8 photoresist deposited onto a polycarbonate beam. The number of layers of MoS₂ is verified using Raman microscopy.²² Titanium clamps are then evaporated through a shadow mask to prevent MoS₂ from slipping against the substrate (Fig. 1a). Uniaxial strain is applied to MoS₂ by controllably bending the polycarbonate beam in a four-point bending apparatus (Fig. 1c,d). Assuming that as-fabricated exfoliated devices before bending are virtually strain-free,²³ we can calculate that upon bending the substrate with radius of curvature R , the induced strain in these devices is $\epsilon = \tau/R$, where $2\tau = 2\text{--}3 \text{ mm}$ is the thickness of the substrate (Fig. 1b).¹² Overall, we fabricated four monolayer and three bilayer MoS₂ devices. The strained devices are probed with a confocal microscope (Thermo Scientific DXR) that is used to collect both Raman

and photoluminescence spectra. We employ a 532nm laser excitation source with average power $\sim 100 \mu\text{W}$, which does not damage our samples.

We first investigate the evolution of the Raman spectra of MoS_2 with strain (Fig. 2). In unstrained monolayer MoS_2 devices, consistent with previous reports,^{22,24} we observe the A' mode due to out-of-plane vibrations at 403 cm^{-1} and the doubly degenerate E' mode due to in-plane vibrations of the crystal at 384 cm^{-1} .

With increased strain, the A' peak shows no measurable shift in position while the degenerate E' peak splits into two subpeaks (in contrast to a previous report²⁵) that we label as E'^+ and E'^- (Fig. 2), as strain breaks the symmetry of the crystal. The A' mode maintains its intensity as strain increases, while the total integrated intensity of the E' peaks now splits between the E'^+ and E'^- peaks. The E'^- peak shifts by $4.5 \pm 0.3 \text{ cm}^{-1}/\%$ strain for monolayer devices and $4.6 \pm 0.4 \text{ cm}^{-1}/\%$ strain for bilayer devices, while the E'^+ peak shifts by $1.0 \pm 1 \text{ cm}^{-1}/\%$ strain for monolayer devices and $1.0 \pm 0.9 \text{ cm}^{-1}/\%$ strain for bilayer devices, consistent with our first-principles calculations (dashed lines in Fig. 2; details of the calculations can be found in the supplementary materials). For applied strain in the range 0–2%, the peak positions shift at nearly identical rates for all measured devices and do not exhibit hysteresis in multiple loading/unloading cycles, indicating that MoS_2 does not slip against the substrate and that the strain does not generate a significant number of defects. Bilayer devices behave in a similar manner but fail, either due to breaking or slipping of the MoS_2 , at strains larger than 1%.

The strain dependence of the Raman E' mode enables us to calculate parameters characterizing anharmonicity of molecular potentials, the Grüneisen parameter, γ , and the shear deformation potential, β :

$$\gamma_{E'} = -\frac{\Delta\omega_{E'^+} + \Delta\omega_{E'^-}}{2\omega_{E'}(1-\nu)\epsilon} \quad (1)$$

$$\beta_{E'} = \frac{\Delta\omega_{E'^+} - \Delta\omega_{E'^-}}{\omega_{E'}(1+\nu)\epsilon} \quad (2)$$

Here ω is the frequency of the Raman mode, $\Delta\omega$ is the change of frequency per unit strain, and ν is Poisson's ratio, which for a material adhering to a substrate is the Poisson ratio of the substrate,

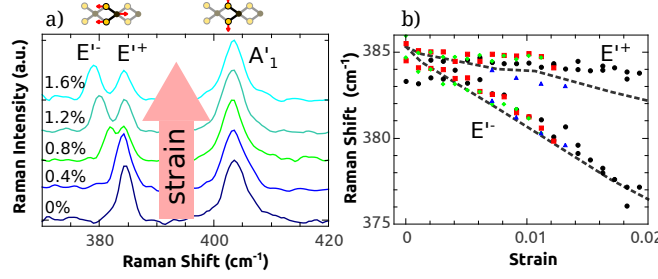


Figure 2: **Phonon softening of single layer MoS₂** (a) Evolution of the Raman spectrum as a device is strained from 0 to 1.6%. (b) The peak location of the the E'^+ and E'^- Raman modes, extracted by fitting the peaks to a Lorentzian, as their degeneracy is broken by straining MoS₂. Different colors represent individual devices. Dashed lines are the results of our first-principles calculations after subtraction of 9 cm^{-1} to account for underestimating phonon energies.

0.33.¹² This yields a Grüneisen parameter of 1.1 ± 0.2 , half that of graphene (1.99)¹² and comparable to that of hexagonal boron nitride (0.95–1.2).^{26,27} The shear deformation potential is 0.78 ± 0.1 for both monolayer and bilayer MoS₂.

Next, we investigate the evolution of the band structure of MoS₂ with strain through photoluminescence (PL) spectroscopy. The principal PL peak (A peak) in unstrained direct-gap monolayer MoS₂ at $1.82 \pm 0.02 \text{ eV}$ (Fig. 3a) is due to a direct transition at the K point (Fig. 3a, inset).^{2,3} The B peak, due to a direct transition between the conduction band and a lower lying valence band, is obscured in our devices by background PL of polycarbonate/SU8. The PL spectra of unstrained indirect-band gap bilayer MoS₂ devices are characterized by a similar A peak at $1.81 \pm 0.02 \text{ eV}$ that originates from the same direct transition, but that is now less intense as it originates from hot luminescence. In addition, we observe an I peak at $1.53 \pm 0.03 \text{ eV}$ (Fig. 3c), which originates from the transition across the indirect band gap of bilayer MoS₂ between the Γ and K points, (Fig. 3c, inset).

Applied strain significantly changes the PL spectra (Fig. 3a,c). For all measured monolayer devices, the A peak redshifts approximately linearly with strain, at a rate of $45 \pm 7 \text{ meV}/\%$ strain (Fig. 3b). For bilayer devices, the A and I peaks are redshifted by 53 ± 10 and $129 \pm 20 \text{ meV}/\%$ strain respectively (Fig. 3d). While the intensity of the A peak in monolayer devices decreases to a third of its original size with an applied strain of 2%, in bilayer devices the intensity of this peak is virtually strain-independent (Figs. 4a).

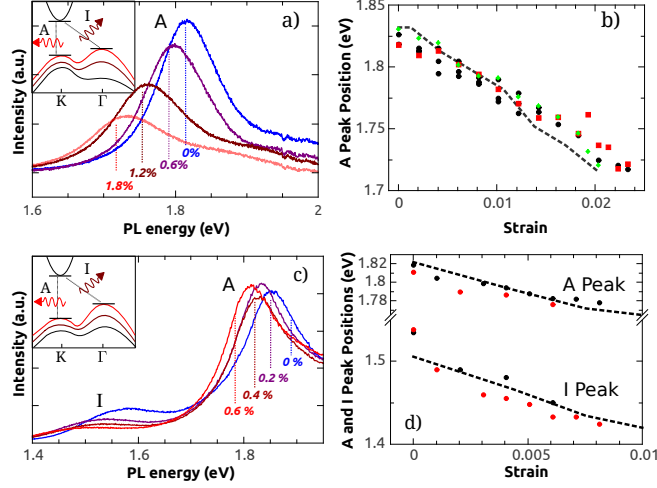


Figure 3: **Photoluminescence spectra of strained MoS₂** (a) PL spectra of a representative monolayer device as it is strained from 0 to 1.8%. Strain independent PL background was subtracted. (b) Evolution of the position of the A peak of the PL spectrum (Lorentzian fits) with strain for several monolayer devices (colors represent different devices) with GW₀-BSE calculations (dashed line) of expected peak position after 25 meV offset. (c) PL spectra of a representative bilayer device as strain is increased from 0 to 0.6%. (d) PL peak position versus strain for the A and I peaks of bilayer devices (colors represent different devices) with good agreement to our GW₀-BSE calculations (dashed lines). Insets in (a) and (b) contains schematic representations of the band structure for both monolayer and bilayer MoS₂ devices that are progressively strained from 0% (black) to ~5% (maroon) and ~8% (red).

To understand our experimental results, we compare them to the results of GW₀-BSE calculations; details are given in supplementary materials. Crucially, these calculations capture the effect of strong electron-electron interactions in MoS₂ leading to the formation of excitons with binding energies significantly exceeding $k_B T$ at room temperature.^{28,29} This is important because PL spectroscopy probes the optical band gap, the difference between the fundamental (or transport) band gap and the exciton binding energy.

The observed redshift of the PL peaks is indicative of strain-induced reduction of band gaps in both monolayer and bilayer MoS₂. Indeed, our GW₀-BSE calculations for a monolayer predict a reduction of the optical band gap at a rate of ~59 meV/% strain (dashed line in Fig. 3b), in close agreement with the measured PL peak shift. In bilayer devices, the calculated rates of reduction for the direct (67 meV/% strain) and indirect (94 meV/% strain) optical band gaps (dashed lines in Fig. 3d) are also in close agreement with measured redshift rates for A and I peaks, 53 ± 10 and

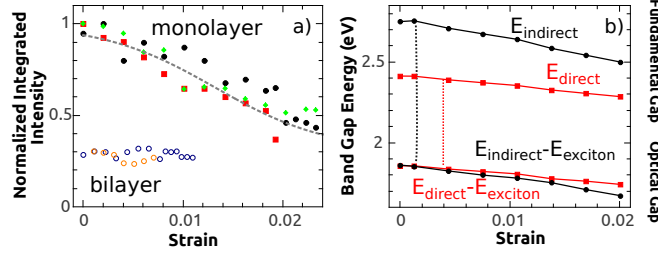


Figure 4: **Direct to indirect band gap transition in MoS₂** (a) Evolution of intensity of the A peak of strained monolayer MoS₂ (solid shapes) with a fit (dashed curve) to the rate equations consistent with a degenerate direct and indirect optical band gap at $1.3 \pm 0.6\%$ strain (supplementary material). PL intensity of bilayer A peak (unfilled circles) with no measurable change in intensity. Each color represents a distinct device. (b) GW₀ calculations of the fundamental band gaps of strained monolayer MoS₂, with an expected degeneracy at $\sim 5\%$ strain. Optical band gap calculated by including the exciton binding energy yields a degeneracy at $\sim 0.1\%$.

129 ± 20 meV/% strain respectively.

We interpret the rapid decrease in PL intensity of monolayer MoS₂ with strain as a signature of the anticipated strain-induced transformation of the *optical* band gap of this material from direct to indirect.^{13,14,18,19} Indeed, at zero strain the energy difference between the minimum of the conduction band at the *K* point and the local maximum of the valence band at the Γ point (the indirect gap) is higher in energy than the direct gap at the *K* point (Fig. 3a, inset, black curve). However, we calculate that the indirect gap reduces with strain faster than the direct gap (59 vs. 94 meV/% strain). As a result, if we ignore the effect of excitons, at $\varepsilon \sim 5\%$ the indirect gap overtakes the direct gap and monolayer MoS₂ becomes an indirect-gap material. With excitonic effects included, our calculations indicate that the direct and indirect *optical* gaps (fundamental gaps minus binding energy of corresponding excitons) become degenerate at a much lower strain, 0.1% (Fig. 4b). We however note that the accuracy of this value sensitively depends on the precise binding energy of the direct and indirect excitons that have not yet been measured experimentally.

As monolayer MoS₂ is strained and transitions from a direct to an indirect band gap material, we expect a marked decrease in the intensity of the A peak, as a majority of the excitons would not reside in this higher energy excitonic state, in good agreement the decrease in intensity in Fig. 4a. Quantitatively, a simple model describing direct and indirect excitons in monolayer MoS₂ as a two-level system yields an acceptable fit to our experimental data (dashed curve in Fig. 4a), with a

direct-to-indirect band gap transition at $1.3 \pm 0.6\%$ strain (details in supplementary information).

The observed PL spectra warrant two more comments. First, while for strains where the indirect band gap of monolayer MoS₂ is lower in energy than the direct band gap, we do not observe a peak corresponding to an indirect transition in its PL spectrum. This is likely due to the much smaller intensity of the indirect photoluminescence compared to the intensity of hot luminescence of the A peak. Second, in the range of strains from 1.3–5%, monolayer MoS₂ enters a curious regime where its fundamental band gap is direct, while the optical band gap is indirect.

In conclusion, we have observed strain-induced phonon softening, band gap modulation and a transition from an optically direct to an optically indirect material in strained MoS₂ samples. These observations support a view of strain engineering as an enabling tool to both explore novel physics in MoS₂ (and other two-dimensional transition metal dichalcogenides such as MoSe₂, WS₂, WSe₂) and to tune its optical and electronic properties. An interesting avenue of research would be to explore the regime of degenerate direct and indirect bands – that play key roles in a plethora of spin-related properties of the MoS₂.^{30,31} Among the potential applications of the strain-dependent photoluminescence of MoS₂ and its cousins are nanoscale stress sensors and tunable photonic devices – LEDs, photodetectors, and electro-optical modulators.

Note: While the manuscript was under review, two studies reporting modification of the band-gap with strain became available.^{32,33} The measured band gap shifts with strain are in general agreement with our results, however due to the much lower range of strains employed in the devices of Ref. [32,33] they do not measure the Grüneisen parameter, probe the direct-to-indirect optical band gap transition, or observe contribution of excitonic effects.

Acknowledgement

This research was supported by NSF DMR-1056859, NSF EPS-1004083, and ONR N000141310299. BW and JZ were supported by DTRA HDTRA1-1-10-1-0047. We thank John Fellenstein for help in designing the four point bending apparatus, Branton Campbell for teaching us about phonon naming conventions, and Ashwin Ramasubramaniam for discussions about the first-principles cal-

culations.

Supporting Information Available: Supporting information, including bilayer Raman data, details of first principles calculations, and a simple two-level model to calculate the intensity of strained MoS₂, is available free of charge via the Internet at <http://pubs.acs.org>.

References

- (1) Wang, Q. H.; Kalantar-Zadeh, K.; Kis, A.; Coleman, J. N.; Strano, M. S. Electronics and optoelectronics of two-dimensional transition metal dichalcogenides. *Nature Nanotechnology* **2012**, *7*, 699–712.
- (2) Mak, K.; Lee, C.; Hone, J.; Shan, J.; Heinz, T. Atomically Thin MoS₂: A New Direct-Gap Semiconductor. *Physical Review Letters* **2010**, *105*, 2–5.
- (3) Splendiani, A.; Sun, L.; Zhang, Y.; Li, T.; Kim, J.; Chim, C.-Y.; Galli, G.; Wang, F. Emerging photoluminescence in monolayer MoS₂. *Nano Letters* **2010**, *10*, 1271–5.
- (4) Radisavljevic, B.; Radenovic, a.; Brivio, J.; Giacometti, V.; Kis, a. Single-layer MoS₂ transistors. *Nature Nanotechnology* **2011**, *6*, 147–50.
- (5) Lin, M.-W.; Liu, L.; Lan, Q.; Tan, X.; Dhindsa, K. S.; Zeng, P.; Naik, V. M.; Cheng, M. M.-C.; Zhou, Z. Mobility enhancement and highly efficient gating of monolayer MoS₂ transistors with polymer electrolyte. *Journal of Physics D: Applied Physics* **2012**, *45*, 345102.
- (6) Yin, Z.; Li, H.; Li, H.; Jiang, L.; Shi, Y.; Sun, Y.; Lu, G. Single-layer MoS₂ phototransistors. *ACS Nano* **2012**, *6*, 74–80.
- (7) Sundaram, R. S.; Engel, M.; Lombardo, A.; Krupke, R.; Ferrari, A. C.; Avouris, P.; Steiner, M. Electroluminescence in Single Layer MoS₂. *Nano Letters* **2013**, *13*, 1416–1421.
- (8) Newaz, A.; Prasai, D.; Ziegler, J.; Caudel, D.; Robinson, S.; Jr., R. H.; Bolotin, K. Electrical control of optical properties of monolayer MoS₂. *Solid State Communications* **2013**, *155*, 49 – 52.

- (9) Ross, J. S.; Wu, S.; Yu, H.; Ghimire, N. J.; Jones, A. M.; Aivazian, G.; Yan, J.; Mandrus, D. G.; Xiao, D.; Yao, W.; Xu, X. Electrical control of neutral and charged excitons in a monolayer semiconductor. *Nature communications* **2013**, *4*, 1474.
- (10) Mak, K. F.; He, K.; Lee, C.; Lee, G. H.; Hone, J.; Heinz, T. F.; Shan, J. Tightly bound trions in monolayer MoS₂. *Nature materials* **2013**, *12*, 207–11.
- (11) Huang, M.; Yan, H.; Chen, C.; Song, D.; Heinz, T. F.; Hone, J. Phonon softening and crystallographic orientation of strained graphene studied by Raman spectroscopy. *Proceedings of the National Academy of Sciences of the United States of America* **2009**, *106*, 7304–8.
- (12) Mohiuddin, T.; Lombardo, a.; Nair, R.; Bonetti, a.; Savini, G.; Jalil, R.; Bonini, N.; Basko, D.; Galotis, C.; Marzari, N.; Novoselov, K.; Geim, a.; Ferrari, a. Uniaxial strain in graphene by Raman spectroscopy: G peak splitting, Grüneisen parameters, and sample orientation. *Physical Review B* **2009**, *79*, 1–8.
- (13) Lu, P.; Wu, X.; Guo, W.; Zeng, X. C. Strain-dependent electronic and magnetic properties of MoS(2) monolayer, bilayer, nanoribbons and nanotubes. *Physical chemistry chemical physics : PCCP* **2012**, *14*, 13035–40.
- (14) Pan, H.; Zhang, Y.-W. Tuning the Electronic and Magnetic Properties of MoS₂ Nanoribbons by Strain Engineering. *The Journal of Physical Chemistry C* **2012**, *116*, 11752–11757.
- (15) Yue, Q.; Kang, J.; Shao, Z.; Zhang, X.; Chang, S.; Wang, G.; Qin, S.; Li, J. Mechanical and electronic properties of monolayer MoS₂ under elastic strain. *Physics Letters A* **2012**, *376*, 1166–1170.
- (16) Li, T. Ideal strength and phonon instability in single-layer MoS₂. *Phys. Rev. B* **2012**, *85*, 235407.
- (17) Scalise, E.; Houssa, M.; Pourtois, G.; Afanas'ev, V.; Stesmans, A. Strain-induced semicon-

- ductor to metal transition in the two-dimensional honeycomb structure of MoS₂. *Nano Research* **2012**, 5, 43–48.
- (18) Shi, H.; Pan, H.; Zhang, Y.-W.; Yakobson, B. I. Quasiparticle band structures and optical properties of strained monolayer MoS₂ and WS₂. *Phys. Rev. B* **2013**, 87, 155304.
- (19) Feng, J.; Qian, X.; Huang, C.; Li, J. Strain-engineered artificial atom as a broad-spectrum solar energy funnel. *Nature Photonics* **2012**, 6, 2–8.
- (20) Bertolazzi, S.; Brivio, J.; Kis, A. Stretching and breaking of ultrathin MoS₂. *ACS Nano* **2011**, 5, 9703–9.
- (21) Novoselov, K. S.; Jiang, D.; Schedin, F.; Booth, T. J.; Khotkevich, V. V.; Morozov, S. V.; Geim, A. K. Two-dimensional atomic crystals. *Proceedings of the National Academy of Sciences of the United States of America* **2005**, 102, 10451–10453.
- (22) Li, H.; Zhang, Q.; Yap, C. C. R.; Tay, B. K.; Edwin, T. H. T.; Olivier, A.; Baillargeat, D. From Bulk to Monolayer MoS₂: Evolution of Raman Scattering. *Advanced Functional Materials* **2012**, 22, 1385–1390.
- (23) Chen, C.; Rosenblatt, S.; Bolotin, K. I.; Kalb, W.; Kim, P.; Kymissis, I.; Stormer, H. L.; Heinz, T. F.; Hone, J. Performance of monolayer graphene nanomechanical resonators with electrical readout. *Nature Nanotechnology* **2009**, 4, 861–7.
- (24) Lee, C.; Yan, H.; Brus, L.; Heinz, T.; Hone, J.; Ryu, S. Anomalous lattice vibrations of single-and few-layer MoS₂. *ACS nano* **2010**, 4, 2695–2700.
- (25) Rice, C.; Young, R. J.; Zan, R.; Bangert, U.; Wolverson, D.; Georgiou, T.; Jalil, R.; Novoselov, K. S. Raman-scattering measurements and first-principles calculations of strain-induced phonon shifts in monolayer MoS₂. *Physical Review B* **2013**, 87, 081307.
- (26) Kern, G.; Kresse, G.; Hafner, J. Ab initio calculation of the lattice dynamics and phase diagram of boron nitride. *Physical Review B* **1999**, 59, 8551–8559.

- (27) Sanjurjo, J. A.; López-Cruz, E.; Vogl, P.; Cardona, M. Dependence on volume of the phonon frequencies and the ir effective charges of several III-V semiconductors. *Phys. Rev. B* **1983**, 28, 4579–4584.
- (28) Cheiwchanchamnangij, T.; Lambrecht, W. R. Quasiparticle band structure calculation of monolayer, bilayer, and bulk MoS₂. *Physical Review B* **2012**, 85, 1–4.
- (29) Ramasubramaniam, A. Large excitonic effects in monolayers of molybdenum and tungsten dichalcogenides. *Phys. Rev. B* **2012**, 86, 115409.
- (30) Mak, K. F.; He, K.; Shan, J.; Heinz, T. F. Control of valley polarization in monolayer MoS₂ by optical helicity. *Nature Nanotechnology* **2012**, 7, 494–498.
- (31) Zeng, H.; Dai, J.; Yao, W.; Xiao, D.; Cui, X. Valley polarization in MoS₂ monolayers by optical pumping. *Nature Nanotechnology* **2012**, 7, 490–3.
- (32) He, K.; Poole, C.; Mak, K. F.; Shan, J. Experimental Demonstration of Continuous Electronic Structure Tuning via Strain in Atomically Thin MoS₂. *Nano Letters* **2013**, 13, 2931–2936.
- (33) Wang, G.; Zhu, C.; Liu, B.; Marie, X.; Feng, Q.; Wu, X.; Fan, H.; Tan, P.; Amand, T.; Urbaszek, B. Strain tuning of optical emission energy and polarization in monolayer and bilayer MoS₂. *arXiv preprint* **2013**, arXiv:1306.3442.